Effects of DHLA-Capped CdSe/ZnS Quantum Dots on the Fibrillation of Human Serum Albumin

Charles H. Vannoy and Roger M. Leblanc*

Department of Chemistry, University of Miami, 1301 Memorial Drive, Coral Gables, Florida 33146-0431

Received: May 19, 2010; Revised Manuscript Received: July 20, 2010

Nanoparticles (NPs) are extremely small in size and possess very large surface areas, which gives them unique properties and applications distinct from those of bulk systems. When exposed to biological fluid, these NPs may become coated with proteins and other biomolecules given their dynamic nature. Hence, there is a significant possibility of an enhanced rate of protein fibrillation by utilizing the NPs as nucleation centers and, thus, promoting fibril formation. Protein fibrillation is closely associated with many fatal human diseases, including neurodegenerative diseases and a variety of systemic amyloidoses. This topic of protein−NP interaction brings about many key issues and concerns, especially with respect to the potential risks to human health and the environment. Herein, we demonstrate the effects of specific NPs, semiconductor quantum dots (QDs), in the process of protein fibril formation from samples of human serum albumin (HSA). The protein−NP systems are analyzed by time-lapse Thioflavin T spectroscopy, Congo red binding assays, circular dichroism (CD), protein fluorescence spectroscopy, and transmission electron microscopy (TEM). Our experimental results illustrate that an increased rate of fibrillation occurs following a thermally activated mechanism in conjunction with the addition of NPs into the protein system. These results give rise to the understanding and possibility of controlling biological self-assembly processes for use in nanobiotechnology and nanomedicine.

Introduction

The rapid growth of the nanotechnology industry has produced a variety of nanomaterials, some of which include inorganic semiconductor nanoparticles (NPs) composed of various elements.[1−3] Subsequent capping of these NPs with organic ligand shells renders them biocompatible and colloidally stable in aqueous mediums.[4−6] These water-soluble NPs possess great potential for use in many nanotechnological and biomedical applications and, thus, have attracted much attention in recent years.[7] However, due to their small size, NPs have the ability to access different areas of the human body, including tissues, cells, and even subcellular organelles.[8−10] The incorporation and accessibility within the human body of these NPs poses a potential biological risk if not properly monitored or controlled. Despite the advances in this emerging field of nanotechnology, little information is known about these potential biological risks from NPs and the mechanisms by which NPs interact with biological systems.[11] Thus, the exposure of NPs to biological fluids composed of biomolecules, more specifically proteins, and the role of these protein−NP interactions in regards to nanotoxicity becomes a concerning issue.[10,12]

Protein aggregation has attracted considerable interest in the fields of materials science and biotechnology due to its association with various diseases, some of which include multiple neurodegenerative diseases and a variety of nonneuropathic systemic amyloidoses.[13−16] To understand the premise behind protein aggregation, one must examine the process of protein misfolding and self-assembly, which creates these highly ordered β-sheet assemblies more commonly known as amyloid fibrils. The fibril formation process originates under conditions in which the native state of the protein is destabilized. Upon partial destabilization or a complete unfolding, the protein follows a mechanism by which relatively short sequence segments with distinct macroscopic structures show a strong tendency to self-aggregate into β-sheet-like assemblies, a process that seems to be a generic feature of polypeptide chains.[14,17,18]

Human serum albumin (HSA) is a physiologically important protein, which happens to be the most abundant protein found in plasma with a normal concentration of approximately 42.0 ± 3.5 g/L, contributing to approximately 60% of the total plasma protein.[19−21] HSA serves as a good model protein for fibrillation studies due to its ability to easily aggregate in vitro despite the fact that native HSA is primarily arranged in an α-helical structure (∼67%), with the remaining protein composition existing as turns and extended or flexible regions,[22] suggesting that HSA has no predisposition to form protein fibrils. Conversely, HSA fibrillation is promoted under different solution conditions such as an increase in the solution temperature, in which partial destabilization of the protein monomers and dimers is favorable.[23,24] The primary sequence of HSA consists of 585 residues in a single polypeptide chain, with a heart-shaped three-dimensional structure that consists of three homologous domains (Figure 1).[19,22,25−27] The protein contains only a single tryptophan residue (Trp^{214}) along with 17 pairs of disulfide bridges and one unpaired cysteine residue (Cys^{34}), which is able to facilitate dimerization of the protein and influence higher-order association.[22,23,25]

In the present work, we have investigated the effect of dihydrolipoic acid-capped CdSe/ZnS QDs (DHLA-capped QDs) having a particle size of roughly 4 nm on the fibrillation of HSA protein. The formation of protein fibrils in the presence of NPs (sizes ranging from 15 to 70 nm) has not been thoroughly studied,[8,9,11,28,29] and only minimal information has been reported involving semiconductor QDs as the NP of choice.[30,31] And while others have successfully studied protein−NP interactions utilizing HSA,[32,33] to the best of our knowledge, there have been no reports on the incorporation of DHLA-capped QDs into the HSA biological system in regards to the rate of protein

* To whom correspondence should be addressed. Phone: (305) 284-2194. Fax: (305) 284-6367. E-mail: rml@miami.edu.

10.1021/jp1045904
Published on Web 08/03/2010

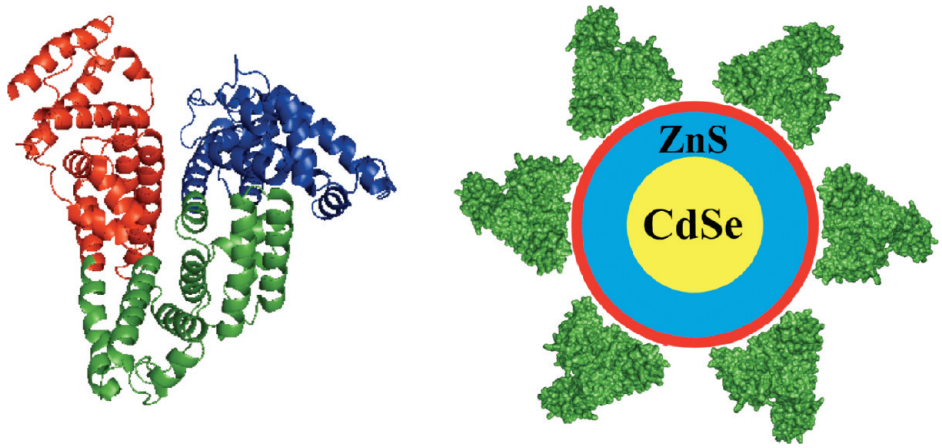

Figure 1. (Left) X-ray crystallographic structure of native HSA.[20] The three constituting domains I, II, and III are represented in blue, green, and red, respectively. (Right) Sketch showing a DHLA-capped CdSe/ZnS QD covered by a monolayer of HSA protein molecules. The organic DHLA layer is represented in red.

fibrillation. It has been suggested that NPs can significantly enhance the rate of protein fibrillation, and essentially the formation of protein fibrils.[8,11] An underlying reasoning suggests that the QDs have the potential to induce HSA fibrillation, due in part to the NP surface charge, which promotes adherence of the HSA protein, as well as the large surface area of the NP, which allows for considerable adsorption capacities (Figure 1).[8,11,28] In this case, the binding of HSA to the DHLA-capped QDs should lead to a significant structural and functional disruption of the HSA molecule. Thus, these nanoscale surfaces of the DHLA-capped QDs act as a nucleation site for HSA molecule association that ultimately promotes oligomer formation, thus, leading to the production of fibrils.[8,11]

Materials and Methods

Materials. All of the listed chemicals were acquired from their respective company at the highest purity available: tetradecylphosphonic acid (TDPA), 98%, Alfa Aesar (Ward Hill, MA); diethyl zinc ($ZnEt_2$), 15 wt % solution in hexane, Acros Organics (Morris Plains, NJ); hexamethyldisilathiane ($(TMS)_2S$), 95%, TCI America (Wellesley Hills, MA); argon, Airgas (Doral, FL); toluene, 100%, Pharmco (Brookfield, CT); HSA, >97%, MP Biomedicals (Solon, OH); and thioflavin T, Calbiochem (La Jolla, CA). All other chemicals and organic solvents were obtained from Sigma-Aldrich (St. Louis, MO) at the highest purity available and used as received. Water utilized for these experiments was obtained from a Modulab 2020 water purification system (Continental Water System Corp., San Antonio, TX). The resistivity and surface tension of the pure water was 18 MΩ·cm and 71.6 mN m^{-1} at 20 °C, respectively.

Synthesis of DHLA-Capped CdSe/ZnS QDs. CdSe/ZnS (core/shell) QDs were synthesized by using a modified technique to previously reported methods[2,34−37] and then surface modified with DHLA according to established protocols giving DHLA-capped QDs with a size of 4.4 ± 0.6 nm in diameter (Supporting Information, Figure S1).[4−6,38]

Preparation of HSA and HSA-QDs Solutions. HSA was dissolved in 1 × PBS buffer (phosphate buffered saline, 137 mM NaCl, 2.7 mM KCl, 10 mM Na_2HPO_4, 2 mM KH_2PO_4, pH 7.4) to make a 10 mg/mL sample of protein solution. All protein solutions were filtered through a 0.20 μm filter into sterile glass vials. DHLA-capped CdSe/ZnS QDs (emission maximum at ca. 570 nm, Supporting Information, Figure S2) at different protein-to-QD molar ratios (1000:1, 2500:1, and 5000:1) are added individually to a 10 mg/mL protein solution. QD concentration was determined spectrophotometrically by using a molar absorption coefficient[39] of ∼1.0 × 10^5 M^{-1} cm^{-1} at ca. 570 nm. A control solution of 10 mg/mL of HSA protein alone was also prepared. The solutions were bath sonicated for a few minutes at room temperature before incubation to facilitate a homogeneous mixture.

Fibrillation Experiments. HSA fibrillation was studied by incubation of the sample solutions prepared in an Autoblot Micro Hybridization Oven (Bellco, Vineland, NJ) at a constant temperature of 65 °C. The length of complete incubation time was 24 h. Portions of the incubated sample solutions were removed periodically and placed in Eppendorf tubes and monitored by characterization experiments. For longer storage before measurement, the Eppendorf tubes with protein samples were frozen at −20 °C. Both freshly prepared and incubated sample solutions were used in all subsequent characterization experiments.

Thioflavin T Spectroscopy. Thioflavin T binding assays were conducted by first preparing a 1 mM Thioflavin T stock solution in 1 × PBS buffer and stored at 4 °C and protected from light until usage. Aliquots of protein solutions were diluted 50-fold into the Thioflavin T stock solution (the final Thioflavin T concentration was 20 μM). Fluorescence was measured with a Horiba Jobin Yvon FluoroLog FL3−22 spectrofluorometer (Horiba Jobin Yvon, Edison, NJ). Fluorescence sample measurements used a quartz cuvette with a 10 mm optical path length. Wavelength measurements were taken from 460 to 700 nm, using an excitation wavelength of 450 nm. Emission and excitation slit widths were typically 5 nm. All fluorescence intensity measurements were background-corrected with a 20 μM Thioflavin T solution that did not contain HSA or HSA-QDs.

Congo Red Binding Assays. Changes in the absorbance of Congo red binding assays were measured with a Perkin-Elmer Lambda 35 UV/vis spectrophotometer (Perkin-Elmer, Norwalk, CT). Aliquots of protein solutions were diluted 50-fold into a 5 μM Congo red buffer solution. UV−vis sample measurements used a quartz cuvette with a 10 mm optical path length. Wavelength measurements were taken from 400 to 700 nm. Absorption spectra of the protein solutions in the presence of the Congo red dye were compared with that of the Congo red buffer alone and the protein solutions in the absence of the Congo red dye.

Circular Dichroism. Far-UV circular dichroism (CD) spectra were obtained with a JASCO J-810 spectropolarimeter. CD

spectra were measured from aliquots withdrawn from the HSA and HSA-QDs aggregation solutions at specific concentrations and incubation times. The CD spectra were recorded between 195 and 250 nm at 25 °C. CD measurements used a quartz cuvette with a 2.0 mm path length.

Protein Fluorescence. The fluorescence emission spectra of HSA and HSA-QDs were taken to analyze the conformational variation of the Trp residue of the HSA protein. Fluorescence was measured with a Horiba Jobin Yvon FluoroLog FL3-22 spectrofluorometer (Horiba Jobin Yvon, Edison, NJ). Fluorescence sample measurements used a quartz cuvette with a 10 mm optical path length. Wavelength measurements were taken from 300 to 500 nm, using an excitation wavelength of 295 nm. Emission and excitation slit widths were typically 5 nm.

Transmission Electron Microscopy (TEM). TEM studies were performed with Formvar/Carbon coated-copper 400 mesh grids (Electron Microscopy Sciences, Hatfield, PA), which were glow discharged and immediately inverted, carbon surface down, onto 5 μL aliquots of HSA and HSA-QDs samples on Parafilm. Samples were diluted 20-fold in 1 × PBS buffer prior to deposition on the grids. Excess liquid was wicked off the grids and immediately placed onto individual droplets of aqueous 2% phosphotungstic acid (PTA), pH 7.0. Excess stain was removed, and the grids were allowed to dry thoroughly. Each sample was examined on a Philips CM100 electron microscope (FEI, Hillsbrough, OR) at 80 kV and images collected with a Megaview III CCD camera (Olympus Soft Imaging Solutions, Lakewood, CO).

Results and Discussion

HSA solutions were incubated with a constant protein concentration of 10 mg/mL in 1 × PBS buffer, pH 7.4, in the absence or presence of varying DHLA-capped QDs concentrations (protein-to-QD molar ratios of 1000:1, 2500:1, and 5000:1) at 65 °C for 24 h, thereby forming complexes with different stoichiometries and creating nanomolar QD concentrations ranging from 150 to 30 nM. High protein-to-QD molar ratios were chosen to ensure a high loading capacity of the HSA protein on the surface of the QDs. Different HSA-QDs ratios were chosen for the purpose of distinguishing any perceptible effects on the rate of aggregation. The choice of using water-soluble DHLA-capped CdSe/ZnS QDs was due to the fact that these types of QDs remain one of the best available components for almost all biological applications and are used extensively in the field of bionanotechnology.[40−42]

It has been previously reported that the α-globular protein HSA has the ability to form fibrils in vitro under various solution conditions (i.e., temperature-induced protein denaturation).[23,24,43] Hence, HSA was subjected to thermal conditions that have been previously shown to be effective in inducing protein aggregation. Thermal conditions at 65 °C were chosen because it is proposed that HSA undergoes a temperature-induced denaturation process through a two-state transition: (1) an initial melting temperature, T_m, of 56.1 ± 0.1 °C and (2) a second T_m of 61.6 ± 0.6 °C. Consequently, there is a sequential unfolding of the protein that takes place between the multiple domains of HSA, more specifically the subdomains IIA and IIIA.[23,24,44] Another factor to consider is hydrogen bonding, a molecular interaction that is weakened by an increase in temperature and disrupts the protein thermal stability. Thus, as the system is subject to these thermal conditions, the initial cooperative hydrogen bonding between the α-helical structures within the protein that once contributed to protein stability eventually begins to break down and leads to the exposure of hydrophobic groups, which promotes a partial unfolding of the protein and presents favorable conditions for fibril formation.[23] As a result, an experimental temperature at 65 °C is assumed to be favorable for protein misfolding and subsequent fibril formation.

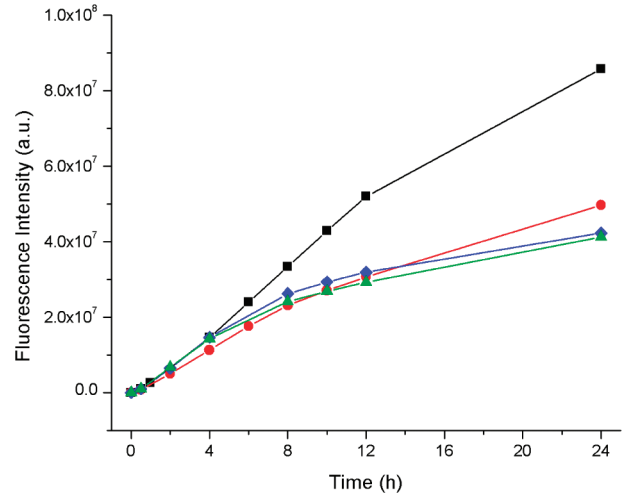

Figure 2. Time evolution of Thioflavin T fluorescence of HSA and HSA-QDs solutions at 65 °C and pH 7.4: (■, black) HSA, (●, red) HSA-QDs (1000:1), (◆, blue) HSA-QDs (2500:1), and (▲, green) HSA-QDs (5000:1).

Fibrillation Kinetics of HSA and HSA-QDs Systems. The ability of HSA and HSA-QDs solutions to form protein aggregates under a thermal condition of 65 °C at physiological pH 7.4 was assessed by tinctorial assays with Thioflavin T and Congo red. These binding assays were conducted by using modified techniques as described in previously reported methods.[21,23,24,45,46] The specific interaction between these organic binding dyes and the HSA fibrils presents a controlled reference and allows for confirmation as to the formation of HSA fibrils. The binding of both of these organic dyes to protein fibrils is highly dependent on the secondary conformation of the protein (i.e., β-pleated sheet).[21,45,46] In addition, both binding assays are a necessity in identifying the presence or absence of protein fibrils, mainly because the affinity of the protein fibrils for Thioflavin T varies and sometimes does not occur with certain protein fibril systems.[47] Thus, the combination of Thioflavin T and Congo red provides a useful tool for the investigation of amyloid-like aggregates in this particular system.

Initially, native HSA at physiological pH does not display a capacity to bind Thioflavin T. However, when the HSA and HSA-QDs systems are subject to thermal conditions of 65 °C, a time-dependent increase in fluorescence is observed (Figure 2). During the early periods of the incubation process, the kinetics of the HSA and HSA-QDs systems exhibit a continuous rising of Thioflavin T fluorescence intensity for both systems. However, closer examination reveals that the HSA-QDs solutions begin to exhibit a discernible lag phase after a short incubation time of 8−12 h, upon which a quasi-plateau region is attained from the time scale analysis. This lag phase is not prominent for the HSA solution in this specific time scale analysis, giving indication that the system is not in alignment with the HSA-QDs systems with regards to producing protein fibrils. Comparably, an initial gelation of the solutions can be observed after a time period of 10 h for the HSA-QDs solutions and 24 h for the HSA solution, indicating an enhanced development of fibril formation and subsequent cross-linkage between the fibrillar moieties. Additionally, there was a noticeable decrease in the Thioflavin T intensity with respect to the HSA-QDs solutions in relation to the HSA solution. There are

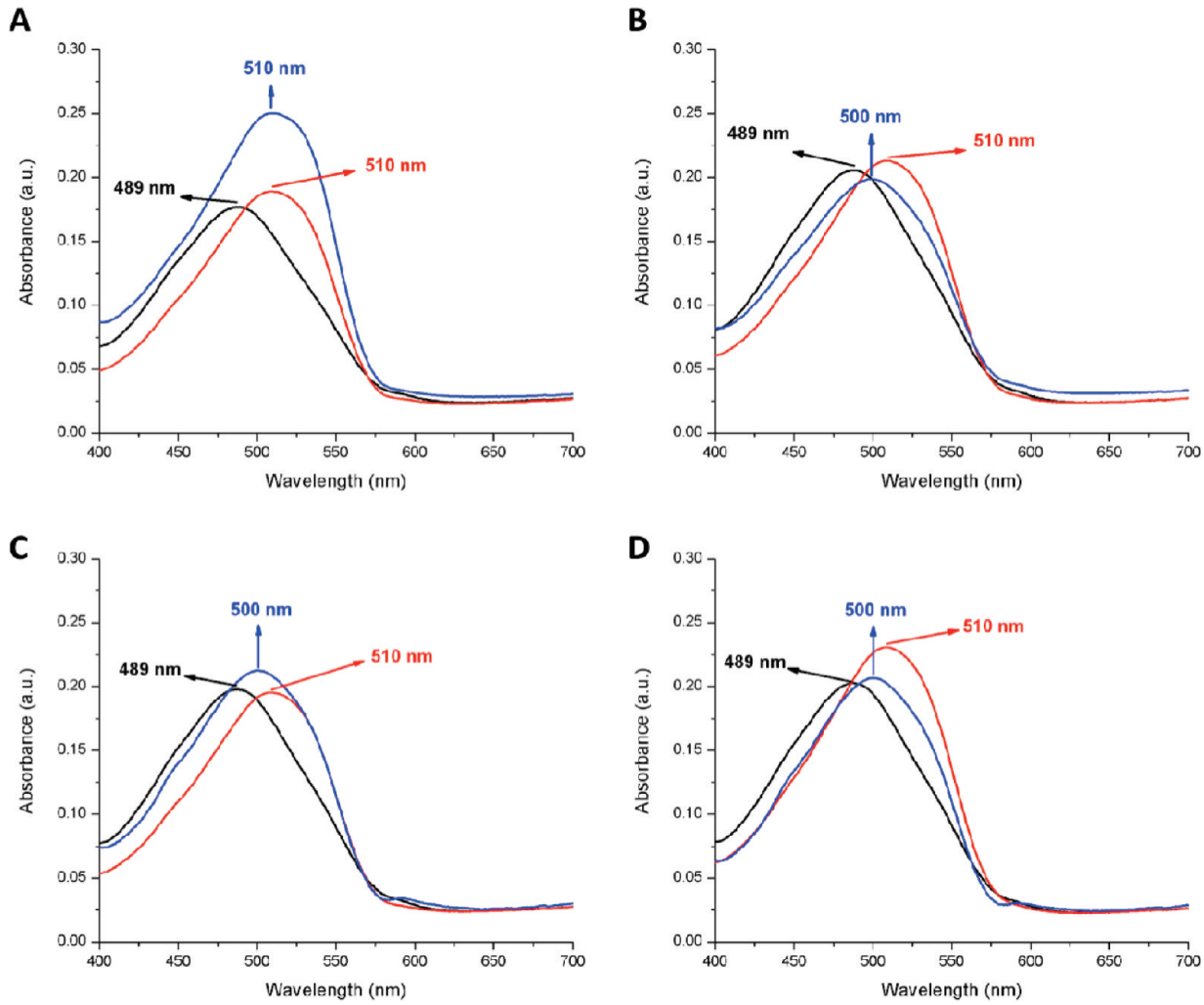

Figure 3. Absorption spectra of Congo Red in HSA and HSA-QDs solutions at 65 °C and pH 7.4: (A) HSA, (B) HSA-QDs (1000:1), (C) HSA-QDs (2500:1), and (D) HSA-QDs (5000:1). Congo Red alone (black) with incubation times of 0 (red) and 10 h (blue).

two possible reasons for this result: (1) there is sufficient energy transfer between the organic fluorophore dye Thioflavin T (donor) and the DHLA-capped QDs (acceptor) or (2) the electrostatic interactions between Thioflavin T and the surface of the DHLA-capped QDs causes a conformational change in the Thioflavin T molecule, thereby altering the binding conformation of Thioflavin T to HSA fibrils. Conclusively, each respective system exhibits an enhancement in fluorescence emission intensity in conjunction with the incorporation of Thioflavin T into the system, which suggests the formation of fibrillar structures. However, the addition of DHLA-capped QDs into the system seems to favor a faster formation of the protein fibrils as indicated by the propensity of Thioflavin T intensity to start leveling off at shorter incubation periods.

Congo red absorption spectra were also analyzed in conjunction with time-evolution Thioflavin T fluorescence to confirm the presence or absence of fibrils in HSA and HSA-QDs solutions. As seen in Figure 3, Congo red alone in buffer gives a maximal absorption peak at ca. 489. However, once Congo red is added to the HSA and HSA-QDs solutions there is a noticeable red-shift in the absorption maximum peak from ca. 489 to ca. 510 nm for all of the solutions at time 0 h. This spectral red-shift may be due in part to the aggregation of Congo red or electrostatic interactions between the sulfonic groups of the Congo red dye molecule and the HSA protein. As the incubation process proceeds and the solutions are subject to the experimental thermal conditions at 65 °C for 10 h, there is an isochromic shift back to ca. 500 nm for the Congo red/HSA-QDs solutions, but not for the Congo red/HSA solution. This result gives an indication that the Congo red dye interacts with the HSA protein in a much different manner at this point, possibly changing the fundamental electronic structure of the system, which suggests that the native HSA protein has converted into a fibrillar form. This result also provides a spectral red-shift in relation to the Congo red dye alone in solution, which suggests that the Congo red molecule binds to the HSA protein fibrils in such a way that it evokes an expansion of the π-electron system of Congo red along with a conformational change in the dye, which may be the reason for the red-shift.[48] Ultimately, these results give an indication that the HSA-QDs solutions have produced protein fibrils after 10 h of incubation, whereas the HSA solution is assumed to still be in a preliminary aggregation process.

Additionally, the subtraction of the experimentally measured absorption spectra for the HSA and HSA-QDs solution in the presence of Congo red and the Congo red solution alone yields difference spectra with maximum peaks of ca. 530 nm and ca. 527 nm for the HSA-QDs solutions and HSA solution, respectively (Supporting Information, Figure S3). With regards to the HSA-QDs solutions with maximum absorption peaks around 530 nm, a result such as this is expected only if well-ordered amyloid-like protein aggregates are present in the

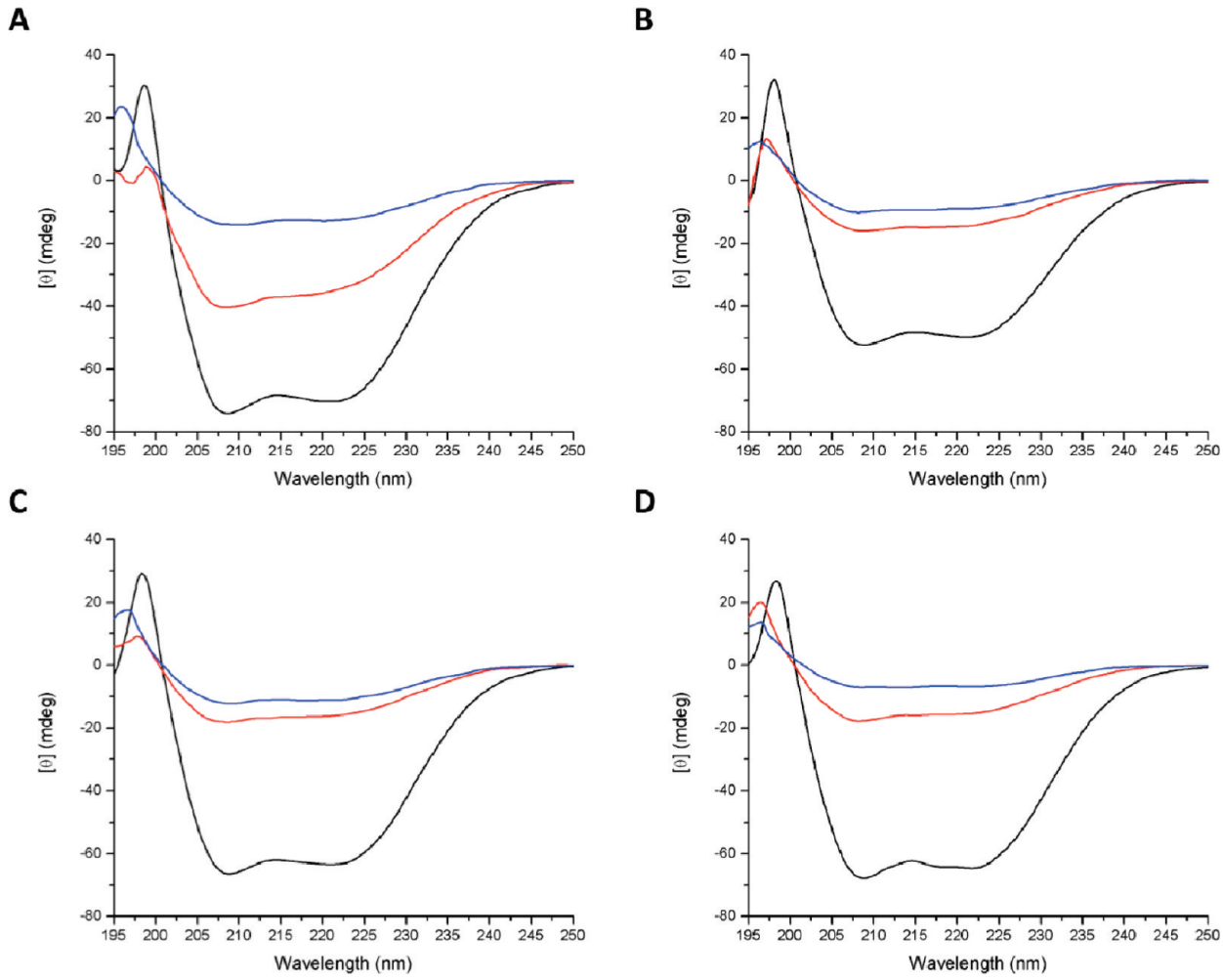

Figure 4. Far-UV spectra of HSA and HSA-QDs solutions at 65 °C and pH 7.4: (A) HSA, (B) HSA-QDs (1000:1), (C) HSA-QDs (2500:1), and (D) HSA-QDs (5000:1) after 0 (black), 10 (red), 24 h (blue).

solutions.[45] This gives a fair indication that the HSA-QDs solutions have produced well-defined protein aggregates, whereas the HSA solution is on course for the same process, but lagging in complete development.

Structural Changes of HSA and HSA-QDs Systems. To examine the differences in fibril formation of HSA in the presence or absence of DHLA-capped QDs with varying concentrations, circular dichroism (CD) and protein (tryptophan, Trp) fluorescence spectra were obtained. The data obtained from these techniques give valuable insight into the protein conformational changes of the HSA and HSA-QDs systems throughout the incubation process.

Figure 4 shows the CD spectra for the HSA and HSA-QDs solutions at 65 °C and pH 7.4 in the absence or presence of varying DHLA-capped QDs concentrations (1000:1; 2500:1; 5000:1). Initially, the far-UV CD spectra produced a positive band around 198 nm and two negative bands at approximately 208 and 222 nm, as well as a crossover point at 201 nm, which resembles that of a regular α-helical structured protein.[49] Upon further analysis of the CD spectra for each solution, a dramatic change in ellipticity is observed throughout the incubation process. Under these specific thermal conditions, the minimums at 208 and 222 nm progressively disappear. This is a strong indication that the experimental conditions give rise to intermediates and final products that are clearly less helical in nature than the initial protein conformations. Consequently, these results suggest that there is an increase in the other secondary structure conformations such as β-sheet and random coil. At longer incubation times (i.e., 10 and 24 h) the CD spectra become more characteristic of a protein with larger proportions of β-sheet structures, which is characterized by a positive band around 196 nm, small $[\theta]$ values, and a negative minimum band

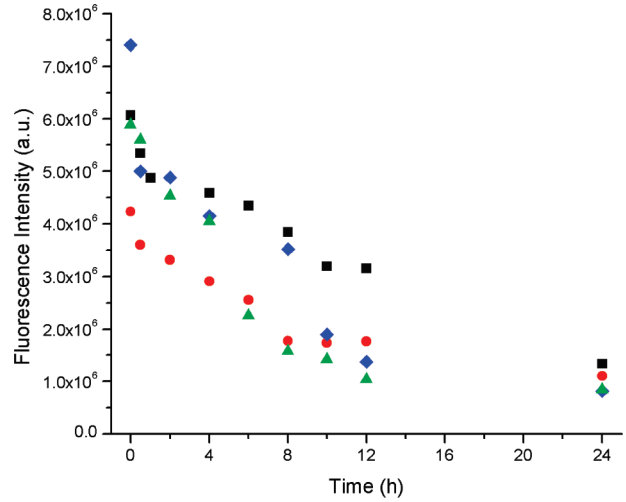

Figure 5. Time evolution of Trp fluorescence maximum intensity of HSA and HSA-QDs solutions at 65 °C and pH 7.4: (■, black) HSA, (●, red) HSA-QDs (1000:1), (◆, blue) HSA-QDs (2500:1), and (▲, green) HSA-QDs (5000:1).

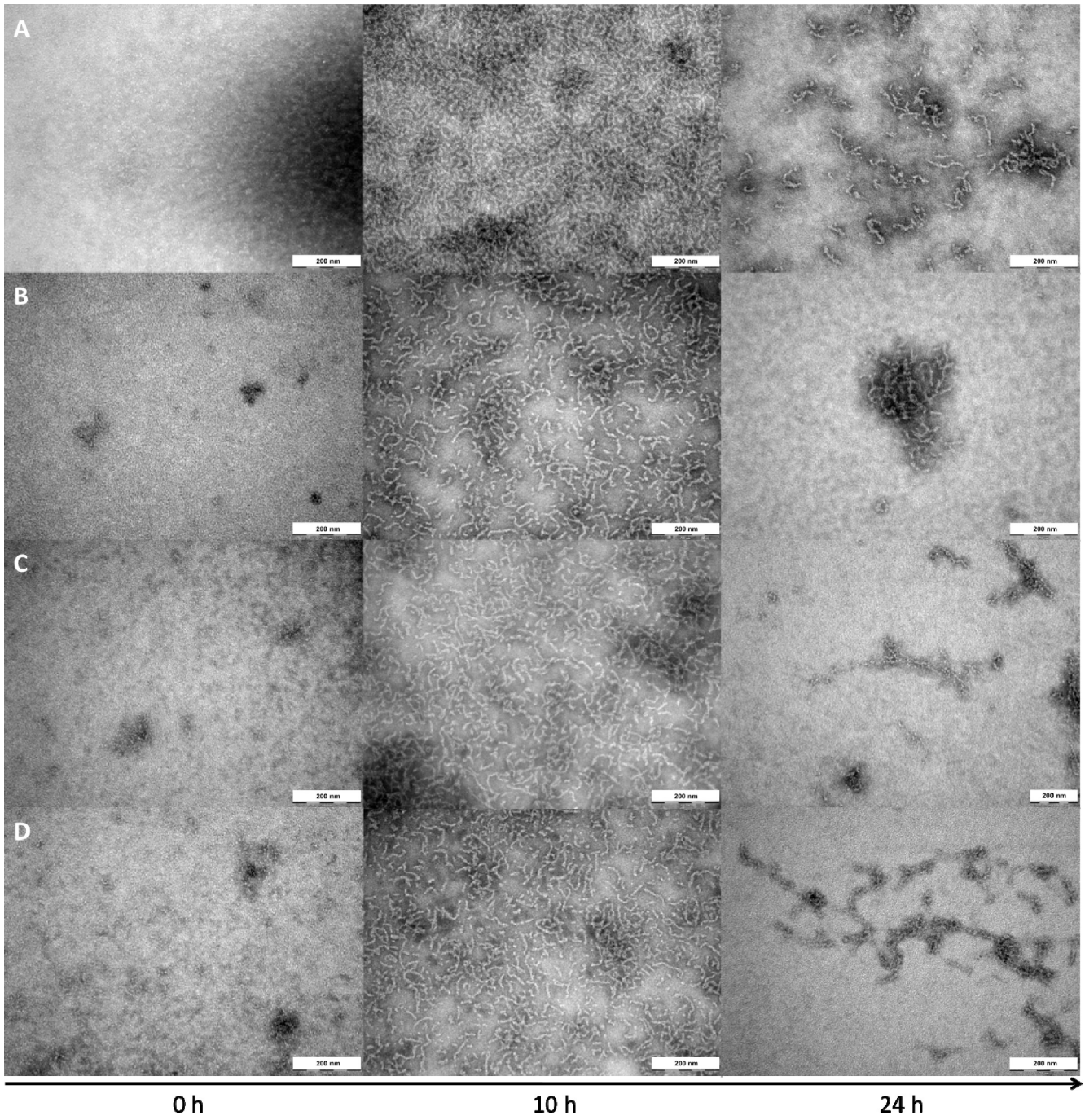

Figure 6. TEM images of (A) HSA, (B) HSA-QDs (1000:1), (C) HSA-QDs (2500:1), and (D) HSA-QDs (5000:1) solutions at 65 °C and pH 7.4 at different stages of the HSA fibrillation process (0, 10, and 24 h).

between 215 and 220 nm.[23,24,49] The most significant change in the far-UV CD spectra that should be pointed out is the fact that these characteristic β-sheet structures are present at earlier incubation times (i.e., 10 h) for the HSA-QDs solutions as opposed to the HSA solution, which shows these characteristic structures at a longer incubation time (i.e., 24 h). This result also helps to substantiate the fact that DHLA-capped QDs promote HSA fibril formation at a faster rate.

The behavior of the HSA-QDs system detailed by the CD measurements is additionally supported by Trp fluorescence data. Despite the size and complexity of HSA, the protein is known to contain only a single Trp residue, Trp^{214}, located in domain II.[19,22] When HSA is in its native state, this Trp^{214} residue is located at the bottom of a 10-Å-wide, 12-Å-deep crevice.[22,23,27] Under the experimental thermal conditions at pH 7.4, the native protein molecule starts to convert into fibrils, thereby initiating an unfolding of domain II in HSA in such a way that the Trp^{214} residue is additionally buried in this crevice and starts to find itself in a more hydrophobic environment.[23,27] This results in a decrease of the Trp fluorescence wavelength emission maximum, λ_{max}, over time (Figure 5). Additionally, there is a hypsochromic shift in the λ_{max} of the Trp fluorescence from ca. 353 nm to ca. 349 nm and the formation of a supplemental peak at ca. 327 nm throughout the incubation process (Supporting Information, Figure S4). The emission spectra of the HSA and HSA-QDs solutions are dependent on the average microenvironment (i.e viscosity, polarity, and interaction of the solvent with the indole ring) around the Trp residue.[50] Initially at time 0 h, there is a spectral characteristic of a Trp residue fully exposed to the aqueous solution. As the incubation process

proceeds, the spectra exhibit systems passing through intermediate conformations resulting from partial exposure of the Trp residue to the aqueous solvent. Finally after 24 h of incubation, the resulting systems show spectral characteristics of a Trp residue located in the interior of HSA, totally isolated from the aqueous solvent. Overall, this decrease in Trp fluorescence intensity and blue shift of the emission maximum give evidence to suggest that there is a strong involvement of the tertiary structures of the domain II of HSA and enhanced intermolecular interactions that give rise to protein fibrillar assemblies.[23,50]

In Situ Observations of HSA and HSA-QDs Systems. TEM images of the HSA and HSA-QDs solutions were recorded at different time intervals throughout the incubation process to distinguish the differences between the samples in relation to the protein aggregates formed (Figure 6). Distinct time-dependent morphological stages can be observed from the TEM images. Before the incubation process begins (0 h) at room temperature, there are no visible signs of any type of aggregates or fibrils present for the HSA and HSA-QDs solutions. However, as the incubation process proceeds to 10 h and the systems are subject to thermal conditions at 65 °C, the HSA-QDs solutions start to develop small, well-defined, short protofibrils with dimensions of ca. 100 nm in length and 4−5 nm in width. Conversely, the HSA solution is devoid of these short protofibril structures, but shows a prolusion for a developing network that is in the process of forming these discrete structures. Upon further incubation of the HSA-QDs solutions, the presence of more elongated fibrils is clearly evident. After 24 h, noticeable fibril formation is observed giving rise to interconnected fibrils with a distinct, curly morphology that reveal macroscopic structures that are >200 nm in length and 8−10 nm in width. Essentially, these elongated structures are produced via several structural intermediates (i.e., short protofibrils) which self-assemble into a bundle of twisted protofibrils, eventually generating more mature fibrils.[51] On the contrary, TEM images of the HSA solutions reveal structures that are reminiscent of the short protofibrils found after an incubation period of 10 h with the HSA-QDs solution. The fibrillar materials produced from these samples appear to be comparable with that of the protofibrils observed at early stages of various amyloidogenic systems. Over time, the thermodynamic instability of the prefibrillar aggregates causes the HSA system to develop into more stable arrangements. This process eventually leads to the formation of discrete fibrils at physiological pH and a temperature of 65 °C. The fibrillation pathway in the presence of varying DHLA-capped QDs concentrations (1000:1; 2500:1; 5000:1) is very similar to that observed in their absence; however, the process seems to take place on a shorter time scale. These results are corroborated with Thioflavin T fluorescence, Congo red binding assays, and CD measurements, which all tend to lead to the same conclusion: incorporation of DHLA-capped QDs into the HSA system significantly enhances the rate of protein fibrillation.

Conclusions

Herein, we analyzed HSA protein fibrillization in vitro with a primary focus on the presence of DHLA-capped QDs in the system and their effect on the self-assembly process. These experiments were conducted under thermal conditions of 65 °C at a physiological pH and with low NP concentrations (≤150 nM). The addition of DHLA-capped QDs into the HSA system led to an acceleration of HSA aggregation and production of protein fibrils, which was independent of the NP nanomolar concentration. On the basis of the results, it is hypothesized that the DHLA-capped QDs ultimately become incorporated into the HSA fibrillar structures. Moreover, the results obtained lead us to substantiate the fact that water-soluble QDs play a key role in protein−NP interactions by acting as a nucleation center and, thus, promoting fibril formation at considerably low NP concentrations. Qualitative studies of protein−NP interactions are still scarce, thus, in order to gain a better understanding on how exactly these NPs interact with biological molecules, more detailed studies must be conducted which focus on how these protein−NP interactions can be controlled and the potential nanotoxicity of NPs in a biological system.

Acknowledgment. This work was supported by the University of Miami, College of Arts & Sciences Bridge funding. We thank Dr. Malcolm Wood at the Core Microscopy Facility (Scripps Research Institute) for technical assistance in TEM observations.

Supporting Information Available: TEM image of DHLA-capped QDs, UV−vis and fluorescence spectra for DHLA-capped QDs, Congo red absorption differences, and fluorescence spectra for Trp fluorescence. This material is available free of charge via the Internet at http://pubs.acs.org.

References and Notes

(1) Alivisatos, A. P. *Science* **1996**, *271*, 933–937.
(2) Hines, M. A.; Guyot-Sionnest, P. *J. Phys. Chem.* **1996**, *100*, 468–471.
(3) Bruchez, M.; Moronne, M.; Gin, P.; Weiss, S.; Alivisatos, A. P. *Science* **1998**, *281*, 2013–2016.
(4) Mattoussi, H.; Mauro, J. M.; Goldman, E. R.; Anderson, G. P.; Sundar, V. C.; Mikulec, F. V.; Bawendi, M. G. *J. Am. Chem. Soc.* **2000**, *122*, 12142–12150.
(5) Clapp, A. R.; Goldman, E. R.; Mattoussi, H. *Nat. Protoc.* **2006**, *1*, 1258–1266.
(6) Algar, W. R.; Krull, U. J. *ChemPhysChem* **2007**, *8*, 561–568.
(7) Sapsford, K. E.; Pons, T.; Medintz, I. L.; Mattoussi, H. *Sensors* **2006**, *6*, 925–953.
(8) Colvin, V. L.; Kulinowski, K. M. *Proc. Natl. Acad. Sci. U.S.A.* **2007**, *104*, 8679–8680.
(9) Wu, W.; Sun, X.; Yu, Y.; Hu, J.; Zhao, L.; Liu, Q.; Zhao, Y.; Li, Y. *Biochem. Biophys. Res. Commun.* **2008**, *373*, 315–318.
(10) Jiang, X.; Weise, S.; Hafner, M.; Röcker, C.; Zhang, F.; Parak, W. J.; Nienhaus, G. H. *J. R. Soc., Interface* **2010**, *7*, S5–S13.
(11) Linse, S.; Cabaleiro-Lago, C.; Xue, W.; Lynch, I.; Lindman, S.; Thulin, E.; Radford, S. E.; Dawson, K. A. *Proc. Natl. Acad. Sci. U.S.A.* **2007**, *104*, 8691–8696.
(12) Lynch, I.; Dawson, K. A. *Nano Today* **2010**, *3*, 40–47.
(13) Stefani, M.; Dobson, C. M. *J. Mol. Med.* **2003**, *81*, 678–699.
(14) Dobson, C. M. *Nature* **2003**, *426*, 884–890.
(15) Chiti, F.; Dobson, C. M. *Annu. Rev. Biochem.* **2006**, *75*, 333–366.
(16) Fändrich, M. *Cell. Mol. Life Sci.* **2007**, *64*, 2066–2078.
(17) Chiti, F.; Taddei, N.; Baroni, F.; Capanni, C.; Stefani, M.; Ramponi, G.; Dobson, C. M. *Nat. Struct. Biol.* **2002**, *9*, 137–143.
(18) Rosseau, F.; Schymkowit, J.; Serrano, L. *Curr. Opin. Struct. Biol.* **2006**, *16*, 118–126.
(19) Peters, T. *Adv. Protein Chem.* **1985**, *37*, 161–245.
(20) Sugio, S.; Kashima, A.; Mochizuki, S.; Noda, M.; Kobayashi, K. *Protein Eng.* **1999**, *12*, 439–446.
(21) Sen, P.; Fatima, S.; Ahmad, B.; Khan, R. H. *Spectrochim. Acta, Part A* **2009**, *74*, 94–99.
(22) Carter, D. C.; Ho, J. X. *Adv. Protein Chem.* **1994**, *45*, 153–203.
(23) Juárez, J.; Taboada, P.; Mosquera, V. *Biophys. J.* **2009**, *96*, 2353–2370.
(24) Juárez, J.; López, S. G.; Cambón, A.; Taboada, P.; Mosquera, V. *J. Phys. Chem. B* **2009**, *113*, 10521–10529.
(25) Brown, J. R. *Serum Albumin: Amino Acid Sequence*; Rosenoer, V. M., Oratz, M., Rothschild, M. A., Eds.; Pergamon: Oxford, UK, 1977.
(26) Flora, K.; Brennan, J. D.; Baker, G. A.; Doody, M. A.; Bright, F. V. *Biophys. J.* **1998**, *75*, 1084–1096.
(27) Qiu, W.; Zhang, L.; Okobiah, O.; Yang, Y.; Wang, L.; Zhong, D. *J. Phys. Chem. B* **2006**, *110*, 10540–10549.
(28) Fei, L.; Perrett, S. *Int. J. Mol. Sci.* **2009**, *10*, 646–655.
(29) Cabaleiro-Lago, C.; Quinlan-Pluck, F.; Lynch, I.; Dawson, K. A.; Linse, S. *ACS Chem. Neurosci.* **2010**, *1*, 279–287.

(30) Roberti, M. J.; Morgan, M.; Menéndez, G.; Pietrasanta, L. I.; Jovin, T. M.; Jares-Erijman, E. A. *J. Am. Chem. Soc.* **2009**, *131*, 8102–8107.
(31) Vannoy, C. H.; Xu, J.; Leblanc, R. M. *J. Phys. Chem. C* **2010**, *114*, 766–773.
(32) Sarkar, R.; Narayanan, S. S.; Pålsson, L.; Dias, F.; Monkman, A.; Pal, S. K. *J. Phys. Chem. B* **2007**, *111*, 12294–12298.
(33) Röcker, C.; Pötzl, M.; Zhang, F.; Parak, W. J.; Nienhaus, G. U. *Nat. Nanotechnol.* **2009**, *4*, 577–580.
(34) Murray, C. B.; Norris, D. J.; Bawendi, M. G. *J. Am. Chem. Soc.* **1993**, *115*, 8706–8715.
(35) Dabbousi, B. O.; Rodriguez-Viejo, J.; Mikulec, F. V.; Heine, J. R.; Mattoussi, H.; Ober, R.; Jensen, K. F.; Bawendi, M. G. *J. Phys. Chem. B* **1997**, *101*, 9463–9475.
(36) Peng, Z. A.; Peng, X. G. *J. Am. Chem. Soc.* **2001**, *123*, 183–184.
(37) Tomasulo, M.; Yildiz, I.; Raymo, F. M. *J. Phys. Chem. B* **2006**, *110*, 3853–3855.
(38) Wagner, A. F.; Walton, E.; Boxer, G. E.; Pruss, M. P.; Holly, F. W.; Folkers, K. *J. Am. Chem. Soc.* **1956**, *78*, 5079–5081.
(39) The molar absorption coefficient was estimated from similar QDs produced from Evident Technologies, Inc.
(40) Murphy, C. J. *Anal. Chem.* **2002**, *74*, 520–526A.
(41) Ozkan, M. *Drug Discovery Today.* **2004**, *9*, 1065–1071.
(42) Michalet, X.; Pinaud, F. F.; Bentolila, L. A.; Tsay, J. M.; Doose, S.; Li, J. J.; Sundaresan, G.; Wu, A. M.; Gambhir, S. S.; Weiss, S. *Science* **2005**, *307*, 538–544.
(43) Taboada, P.; Barbosa, S.; Castro, E.; Mosquera, V. *J. Phys. Chem. B* **2006**, *110*, 20733–20736.
(44) Farruggia, B.; Rodriguez, F.; Rigatuso, R.; Fidelio, G.; Picó, G. *J. Protein Chem.* **2001**, *20*, 81–89.
(45) Klunk, W. E.; Pettegrew, J. W.; Abraham, D. J. *J. Histochem. Cytochem.* **1989**, *37*, 1273–1281.
(46) Levine, H. *Amyloid* **1995**, *2*, 1–6.
(47) Khurana, R.; Coleman, C.; Ionescu-Zanetti, C.; Carter, S. A.; Krishna, V.; Grover, R. K.; Roy, R.; Singh, S. *J. Struct. Biol.* **2005**, *151*, 229–238.
(48) Miura, T.; Yamamiya, C.; Sasaki, M.; Suzuki, K.; Takeuchi, H. *J. Raman Spectrosc.* **2002**, *33*, 530–535.
(49) Sreerama, N.; Venyaminov, S. Y.; Woody, R. W. *Protein Sci.* **1999**, *8*, 370–380.
(50) Santos, N. C.; Castanho, M. *Trends Appl. Spectrosc.* **2002**, *4*, 113–125.
(51) Hamley, I. W. *Angew. Chem., Int. Ed.* **2007**, *46*, 8128–8147.

JP1045904